

# **Li<sub>6</sub>Al<sub>2</sub>Ta<sub>2</sub>O<sub>12</sub> (A=Sr, Ba): Novel Garnet-Like Oxides for Fast Lithium Ion Conduction\*\***

By Venkataraman Thangadurai\* and Werner Weppner

Oxides with the nominal chemical formula Li<sub>6</sub>Al<sub>2</sub>Ta<sub>2</sub>O<sub>12</sub> (A=Sr, Ba) have been prepared via a solid-state reaction in air using high purity La<sub>2</sub>O<sub>3</sub>, LiOH·H<sub>2</sub>O, Sr(NO<sub>3</sub>)<sub>2</sub>, Ba(NO<sub>3</sub>)<sub>2</sub>, and Ta<sub>2</sub>O<sub>5</sub> and are characterized by powder X-ray diffraction (XRD) in order to identify the phase formation and AC impedance to determine the lithium ion conductivity. The powder XRD data of Li<sub>6</sub>Al<sub>2</sub>Ta<sub>2</sub>O<sub>12</sub> show that they are isostructural with the parent garnet-like compound Li<sub>5</sub>La<sub>3</sub>Ta<sub>2</sub>O<sub>12</sub>. The cubic lattice parameter was found to increase with increasing ionic size of the alkaline earth ions (Li<sub>6</sub>SrLa<sub>2</sub>Ta<sub>2</sub>O<sub>12</sub>: 12.808(2) Å; Li<sub>6</sub>BaLa<sub>2</sub>Ta<sub>2</sub>O<sub>12</sub>: 12.946(3) Å). AC impedance results show that both the strontium and barium members exhibit mainly a bulk contribution with a rather small grain-boundary contribution. The ionic conductivity increases with increasing ionic radius of the alkaline earth elements. The barium compound, Li<sub>6</sub>BaLa<sub>2</sub>Ta<sub>2</sub>O<sub>12</sub>, shows the highest ionic conductivity, 4.0×10<sup>-5</sup> S cm<sup>-1</sup> at 22 °C with an activation energy of 0.40 eV, which is comparable to other lithium ion conductors, especially with the presently employed solid electrolyte lithium phosphorus oxynitride (Lipon) for all-solid-state lithium ion batteries. DC electrical measurements using lithium-ion-blocking and reversible electrodes revealed that the electronic conductivity is very small, and a high electrochemical stability (>6 V/Li) was exhibited at room temperature. Interestingly, Li<sub>6</sub>Al<sub>2</sub>Ta<sub>2</sub>O<sub>12</sub> was found to be chemically stable with molten metallic lithium.

## 1. Introduction

Present lithium ion battery technology is based on liquid organic electrolytes, which have several disadvantages and severe problems. These are related to safety concerns because of potential electronic short circuits of the electrodes, formation of reaction product layers at the electrolyte-electrode interfaces ("solid electrolyte interfaces", SEIs), leakage of the liquid, low electrochemical decomposition voltages, and accordingly restrictions with regard to higher energy densities.

Solid-state lithium ion conductors (SSLICs) with the following properties: i) high ionic conductivity with negligible electronic conductivity; ii) long-term chemical stability with electrodes (both anode and cathode), especially in contact with a metallic lithium or lithium alloy anode; and iii) high electrochemical stability ( $\geq 5.5$  V/Li) are expected to replace the currently used liquid electrolyte and allow the use of high voltage cathode materials. So far, all discovered inorganic compounds have either a high ionic conductivity or high electrochemical stability, but not both.<sup>[1-3]</sup> In addition, some of the best lithium ion conductors, for example, Li<sub>3x</sub>La<sub>(2/3)-x</sub>□<sub>1/3</sub>-<sub>2x</sub>TiO<sub>3</sub> (LLT, where □ represents a vacancy) ( $0 < x < 0.16$ ; LLT;  $x \approx 0.1$  exhibits a bulk conductivity of 10<sup>-3</sup> S cm<sup>-1</sup> at 27 °C) become predominantly electronic conductors within the lithium activity range

given by the two electrodes.<sup>[4-6]</sup> Since polycrystalline materials are being used for practical applications, large grain-boundary resistances are commonly observed in addition to the bulk resistance and therefore control the total resistance of the galvanic cells. For instance, LLT exhibits a total (bulk + grain-boundary) conductivity of 7×10<sup>-5</sup> S cm<sup>-1</sup> at 27 °C, which is about two orders of magnitude lower than that of the bulk ionic conductivity.<sup>[4,6]</sup>

Herein, we report for the first time predominant ionic conduction in a garnet-type structure of nominal chemical composition Li<sub>6</sub>Al<sub>2</sub>Ta<sub>2</sub>O<sub>12</sub> (A=Sr, Ba) and show that these new materials overcome the existing problems (i.e., lack of high ionic conductivity with good chemical and electrochemical stability and very low grain-boundary resistance at room temperature). These compounds were found to be stable against reaction with molten elemental lithium, lithium cathodes, and have high decomposition voltages (more than 6 V/Li) at room temperature. The ionic conduction occurs in three dimensions—similar to that of the best, but unstable, known solid lithium electrolytes.

Garnets are orthosilicates with the general structural formula A<sub>3</sub><sup>II</sup>B<sub>2</sub><sup>III</sup>(SiO<sub>4</sub>)<sub>3</sub>, where A and B refer to eight-coordinated and six-coordinated cation sites,<sup>[7]</sup> respectively. SiO<sub>4</sub> tetrahedra are isolated and connected to each other through ionic bonds with the interstitial B-cations. A large variety of complex oxides have also been found to crystallize in garnet-like structures with other elements replacing silicon, for example, A<sub>3</sub>B<sub>5</sub>O<sub>12</sub> (A=Ca, Mg, Y, or Ln=La, or rare earth elements; B=Al, Fe, Ga, Ge, Mn, Ni, V). They are comprised of a three-dimensional framework consisting of BO<sub>6</sub> octahedra and BO<sub>4</sub> tetrahedra, in which each octahedron is joined to six others via corner-sharing tetrahedra. Each tetrahedron shares each corner with four octahedra.<sup>[7]</sup>

[\*] Prof. V. Thangadurai, Prof. W. Weppner  
Sensors and Solid State Ionics, Faculty of Engineering  
University of Kiel, Kaiserstr. 2, D-24143, Kiel (Germany)  
E-mail: vt@tf.uni-kiel.de

[\*\*] Dr. V. Thangadurai thanks the German Academic Exchange Service (DAAD), Bonn, Germany for financial support in the framework of the Guest Professorship program.

Compounds with the chemical formula  $\text{Li}_5\text{La}_3\text{M}_2\text{O}_{12}$  ( $\text{M}=\text{Nb}, \text{Ta}$ ) were found to have a garnet-like structure with the lattice constant  $a=12.889(3)$  Å for niobium and  $a=12.823(2)$  Å for tantalum, and containing an excess of sixteen lithium atoms in the unit cell.<sup>[8,9]</sup> Figure 1 shows the crystal structure of  $\text{Li}_5\text{La}_3\text{M}_2\text{O}_{12}$ . The lanthanum and niobium (tantalum) ions occupy the eight- and six-coordination sites, respectively, and lithium ions occupy the octahedral sites. Among them, one of the “ $\text{Li(I)O}_6$ ” is highly distorted.<sup>[8]</sup> This position turns out to be vacant in a conventional garnet structure with the usual stoichiometry,  $\text{A}_3\text{B}_5\text{O}_{12}$ . The  $\text{MO}_6$  octahedra are surrounded by six lithium ions and two lithium ion vacancies in the parent  $\text{Li}_5\text{La}_3\text{M}_2\text{O}_{12}$ <sup>[8]</sup> molecule and accordingly they show appreciable lithium ion conduction.<sup>[10]</sup>

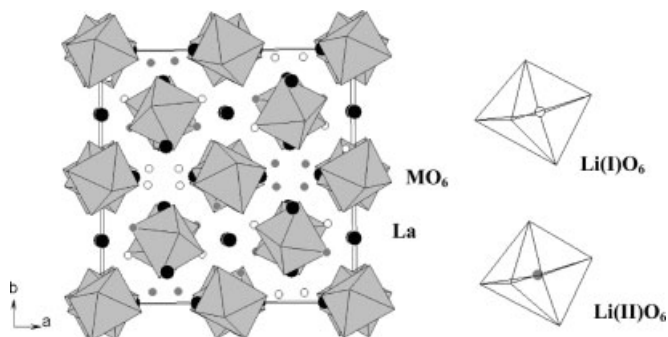


**Figure 1.** Crystal structure of parent garnet-like  $\text{Li}_5\text{La}_3\text{M}_2\text{O}_{12}$  ( $\text{M}=\text{Nb}, \text{Ta}$ ) ( $\text{MO}_6$ : octahedra, lanthanum: large solid circles;  $\text{Li(I)}$ : empty circles;  $\text{Li(II)}$ : small solid circles) [8]. The lithium's oxygen coordination environment is shown on the right-hand side.

## 2. Results and Discussion

### 2.1. Structure Description

Figure 2 shows the measured and calculated powder XRD patterns of  $\text{Li}_6\text{Al}_2\text{Ta}_2\text{O}_{12}$  ( $\text{A}=\text{Sr}, \text{Ba}$ ) together with the corresponding data of the parent compound  $\text{Li}_5\text{La}_3\text{Ta}_2\text{O}_{12}$ . The powder XRD patterns for  $\text{Li}_5\text{La}_3\text{Ta}_2\text{O}_{12}$  (Fig. 2a) and  $\text{Li}_6\text{Al}_2\text{Ta}_2\text{O}_{12}$  (Fig. 2c for strontium; Fig. 2e for barium) were calculated using the atomic positions from single crystal data employing the Powder Cell program.<sup>[11]</sup> For the calculation of  $\text{Li}_6\text{Al}_2\text{Ta}_2\text{O}_{12}$  patterns, we replaced the alkaline earth ions at the lanthanum sites (12b) and the excess lithium was included at the partially occupied  $\text{Li}(1)$ -site (24c) in the same space group  $I\bar{2}3$ . We see that all the measured lines match those of the parent compound, indicating that the compounds are isostructural. We plan to perform neutron diffraction studies to confirm the position of the excess lithium ions. As expected, the cubic lattice constant increases with increasing size of the alkaline earth ions ( $\text{Li}_6\text{SrLa}_2\text{Ta}_2\text{O}_{12}$ : 12.808(2) Å;  $\text{Li}_6\text{BaLa}_2\text{Ta}_2\text{O}_{12}$ : 12.946(3) Å). The eight-fold coordination ionic radius for  $\text{Sr}^{2+}$  is 1.25 Å and for  $\text{Ba}^{2+}$  1.42 Å. The corresponding value for  $\text{La}^{3+}$  ion is 1.18 Å.<sup>[12]</sup>

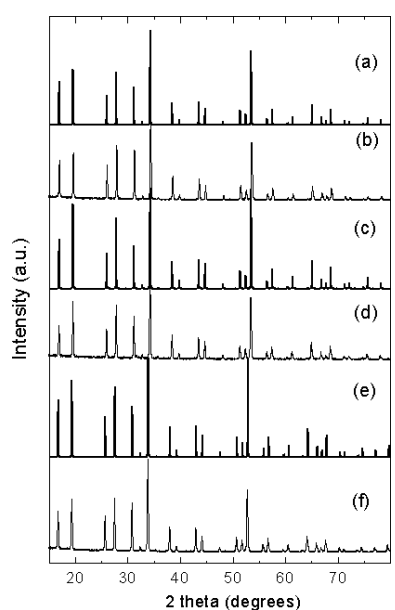


**Figure 2.** Powder XRD patterns of a)  $\text{Li}_5\text{La}_3\text{Ta}_2\text{O}_{12}$  (calculated), b)  $\text{Li}_5\text{La}_3\text{Ta}_2\text{O}_{12}$  (measured), c)  $\text{Li}_6\text{SrLa}_2\text{Ta}_2\text{O}_{12}$  (calculated), d)  $\text{Li}_6\text{SrLa}_2\text{Ta}_2\text{O}_{12}$  (measured), e)  $\text{Li}_6\text{BaLa}_2\text{Ta}_2\text{O}_{12}$  (calculated), and f)  $\text{Li}_6\text{BaLa}_2\text{Ta}_2\text{O}_{12}$  (measured). The powder patterns ( $\text{Cu K}\alpha$ ) were calculated using the single crystal structure data reported in the literature for  $\text{Li}_5\text{La}_3\text{Ta}_2\text{O}_{12}$  [8].

### 2.2. Electrical Properties

#### 2.2.1. Alternating Current (AC) Impedance

Typical impedance plots of  $\text{Li}_6\text{SrLa}_2\text{Ta}_2\text{O}_{12}$  at 22 and 100 °C in air are shown in Figure 3. The low-temperature impedance plots could be well-resolved into bulk, grain-boundary, and

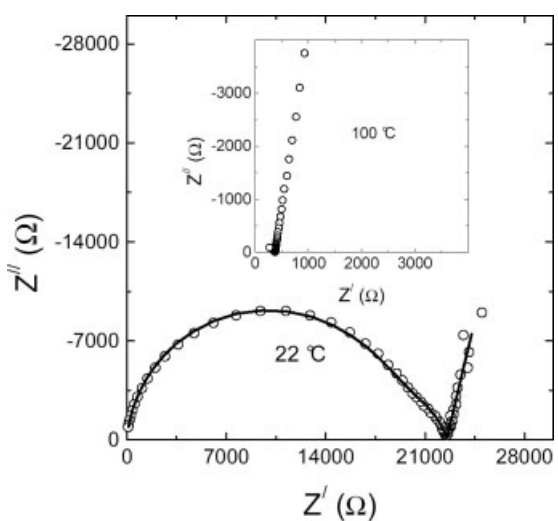


**Figure 3.** AC impedance plots measured in air for  $\text{Li}_6\text{SrLa}_2\text{Ta}_2\text{O}_{12}$  at 22 and 100 °C using lithium-ion-blocking electrodes. The empty circles are measured data and the solid line represents the simulated data using the EQUIVALENT program [13] with an equivalent circuit consisting of two parallel resistance-capacitance and capacitance contributions ( $R_b C_b$ ) ( $R_{gb} C_{gb}$ ) ( $C_e$ ). The appearance of a tail at the low frequency side indicates the blocking nature for mobile lithium ions and is evidence that the garnet-type materials are ionic conductors [14,15].

electrode effects. The solid line represents fitted data with an equivalent circuit consisting of two parallel resistance–capacitance and capacitance contributions ( $R_b C_b$ ) ( $R_{gb} C_{gb}$ ) ( $C_{el}$ ) using the EQUIVALENT program.<sup>[13]</sup> It is similar to that of other fast lithium ion conductors, such as LLT and  $\beta$ -aluminas. The appearance of a tail at the low frequency side suggests the blocking of the electrodes for the mobile ions (lithium).<sup>[14,15]</sup> Table 1 lists the impedance data at 22 °C for  $\text{Li}_6\text{AlA}_2\text{Ta}_2\text{O}_{12}$  (A=Sr, Ba). The grain-boundary contribution decreases with increasing temperature. Above 70 °C, it is difficult to separate each contribution; accordingly, we have considered the total (bulk + grain-boundary) contribution for determining the electrical conductivity over the temperature range investigated.

**Table 1.** Impedance data of  $\text{Li}_6\text{AlA}_2\text{Ta}_2\text{O}_{12}$  (A=Sr, Ba) at 22 °C in air.

Compound	$R_{\text{bulk}}$ [kΩ]	$C_{\text{bulk}}$ [F]	$R_{\text{gb}}$ [kΩ]	$C_{\text{gb}}$ [F]	$C_{\text{el}}$ [F]	$\sigma_{\text{total}}$ [S cm <sup>-1</sup> ]	$E_a$ [eV]
$\text{Li}_6\text{SrLa}_2\text{Ta}_2\text{O}_{12}$	18.83	$3.0 \times 10^{-11}$	3.68	$8.5 \times 10^{-9}$	$5.7 \times 10^{-6}$	$7.0 \times 10^{-6}$	0.50
$\text{Li}_6\text{BaLa}_2\text{Ta}_2\text{O}_{12}$	3.45	$1.2 \times 10^{-10}$	1.34	$1.3 \times 10^{-7}$	$1.2 \times 10^{-6}$	$4.0 \times 10^{-5}$	0.40

### 2.2.2. Total Electrical Conductivity

The Arrhenius plots for the total (bulk + grain-boundary) electrical conductivity of  $\text{Li}_6\text{AlA}_2\text{Ta}_2\text{O}_{12}$  (A=Sr, Ba) are shown in Figure 4. The data obtained from two heating and cooling cycles follow the same line with activation energies of 0.50 and 0.40 eV for  $\text{Li}_6\text{SrLa}_2\text{Ta}_2\text{O}_{12}$  and  $\text{Li}_6\text{BaLa}_2\text{Ta}_2\text{O}_{12}$ , respectively.  $\text{Li}_6\text{BaLa}_2\text{Ta}_2\text{O}_{12}$  ( $4.0 \times 10^{-5}$  S cm<sup>-1</sup>) exhibits a higher total conductivity than that of  $\text{Li}_6\text{SrLa}_2\text{Ta}_2\text{O}_{12}$  ( $7.0 \times 10^{-6}$  S cm<sup>-1</sup>) at 22 °C (Table 1). It must be mentioned that total and bulk conductivities are nearly the same magnitude for the presently investigated garnet-type materials. For example, the strontium and barium compounds exhibit bulk ionic

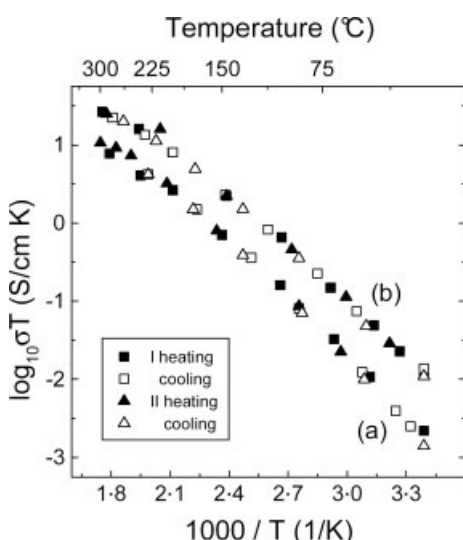


**Figure 4.** Arrhenius plots for the total (bulk + grain-boundary) lithium ion conductivity of a)  $\text{Li}_6\text{SrLa}_2\text{Ta}_2\text{O}_{12}$  and b)  $\text{Li}_6\text{BaLa}_2\text{Ta}_2\text{O}_{12}$ . The data were obtained from two heating and cooling cycles and follow the same line.

conductivities of  $8.84 \times 10^{-6}$  S cm<sup>-1</sup> and  $5.38 \times 10^{-5}$  S cm<sup>-1</sup>, respectively at 22 °C. This finding is a most attractive feature of the investigated garnet-type oxides compared to other ceramic lithium ion conductors. For comparison, the best lithium ion conductor based on perovskite LLT exhibits a total conductivity about two orders of magnitude lower than that of the bulk conductivity.<sup>[4,6]</sup>

Figure 5 shows a comparison of the lithium ion conductivity of  $\text{Li}_6\text{BaLa}_2\text{Ta}_2\text{O}_{12}$  with that of other lithium ion conductors reported in the literature. The conductivity is higher than in the case of  $\text{Li}\beta\text{-alumina}$ ,<sup>[16]</sup> thin film LIPON ( $\text{Li}_{2.9}\text{PO}_{3.3}\text{N}_{0.46}$ ),<sup>[17]</sup>  $\text{Li}_9\text{SiAlO}_8$ ,<sup>[18]</sup>  $\text{LiI} + 40\text{ mol Al}_2\text{O}_3$ ,<sup>[19]</sup>  $\text{LiZr}_2(\text{PO}_4)_3$ ,<sup>[20]</sup>  $\text{Li}_{3.5}\text{Si}_{0.5}\text{P}_{0.5}\text{O}_4$ ,<sup>[21]</sup> and  $\text{Li}_5\text{La}_3\text{Ta}_2\text{O}_{12}$ ,<sup>[10]</sup> and is comparable to that of the rather unstable  $\text{Li}_3\text{N}$  (0.45 V) and  $\text{Li}_{3.5}\text{Si}_{0.5}\text{P}_{0.5}\text{O}_4$  at high temperature, however, at room temperature  $\text{Li}_3\text{N}$  has a conductivity an order of magnitude higher.<sup>[2,3]</sup> The high ionic conductivity in the present class of materials is believed to be due to the migration of lithium ions through interstitial sites. This is different from most lithium ion conductors<sup>[1,3–5]</sup> known so far. In contrast to  $\text{Li}\beta\text{-alumina}$  and  $\text{Li}_3\text{N}$ , the garnet is an isotropic compound and hence the conductivity occurs in three dimensions.

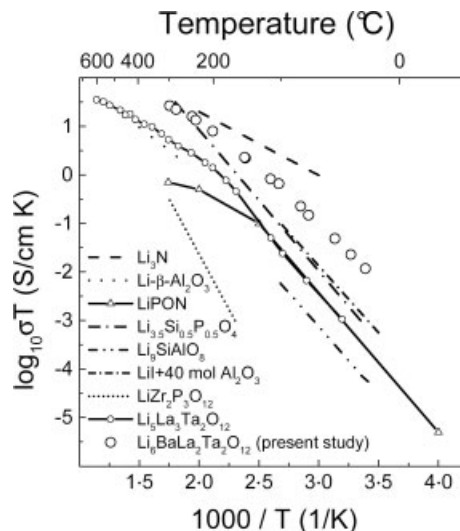


**Figure 5.** Comparison of total (bulk + grain-boundary) lithium ion conductivity of  $\text{Li}_6\text{BaLa}_2\text{Ta}_2\text{O}_{12}$  with other lithium ion conductors reported in the literature.

### 2.2.3. Hebb–Wagner Polarization Study

In Figure 6, we show the Hebb–Wagner (HW) polarization data at 22 °C and 44 °C, obtained using metallic lithium as the reference electrode (activity of lithium,  $a_{\text{Li}} = 1$ ) and a gold lithium-ion-blocking electrode. As the lithium ions are blocked, the steady-state current is due to electrons and holes only.<sup>[22,23]</sup> The steady-state electronic current was of the order of  $10^{-7}$  A. Very interestingly, we did not see an exponential increase in current up to 6 V/Li, indicating that  $\text{Li}_6\text{BaLa}_2\text{Ta}_2\text{O}_{12}$  is highly electrochemically stable (no decomposition). This result is

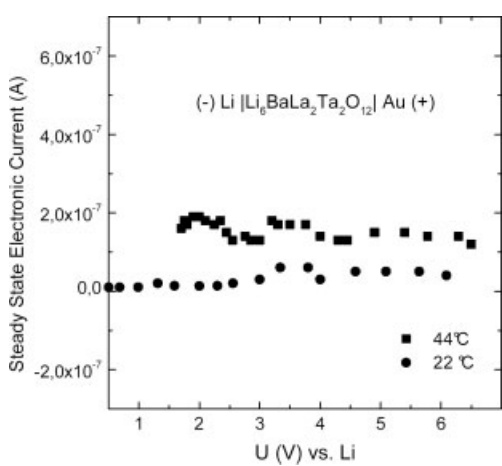


**Figure 6.** Steady-state electronic current as a function of applied voltage for  $\text{Li}_6\text{BaLa}_2\text{Ta}_2\text{O}_{12}$ , obtained at 22 °C and 44 °C by Hebb-Wagner (HW) measurements with a lithium-ion-blocking electrode and using elemental lithium as the reference electrode. The measurements were performed inside an argon-filled glove box with an oxygen partial pressure of less than 1 ppm.

consistent with DC measurements with a lithium-ion-blocking gold electrode and the magnitude of the steady-state electronic current is of the same (slightly lower) order of magnitude. The estimated electronic conductivity is in the range  $<10^{-7}$ – $10^{-6} \text{ S cm}^{-1}$  (22–44 °C) at an activity of lithium of one, which is about two orders of magnitude lower than that of the total conductivity (Fig. 4). The transference number of lithium was found to be close to one ( $t_{\text{Li}} = (\sigma_{\text{total}} - \sigma_{\text{electronic}})/\sigma_{\text{total}} \approx 1$ ). The AC impedance value was taken as the total conductivity ( $\sigma_{\text{total}} = 4.0 \times 10^{-5} \text{ S cm}^{-1}$  at 22 °C).

Using reversible metallic lithium as the electrodes,  $\text{Li}_6\text{AlA}_2\text{Ta}_2\text{O}_{12}$  ( $\text{A}=\text{Sr}, \text{Ba}$ ) shows a single semicircle with a total resistance of 22.5 kΩ for the strontium and 7.5 kΩ for the barium compound at 23 °C (Fig. 7). The appearance of the low-frequency intercept in this case is a second—and more definite—indication of lithium ion conduction in the investigated garnet-type materials.<sup>[14,15]</sup> While using a lithium-ion-blocking electrode, we observed a tail in the low frequency side due to

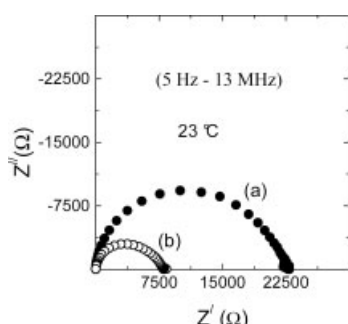


**Figure 7.** AC impedance plots recorded at 23 °C for a)  $\text{Li}_6\text{SrLa}_2\text{Ta}_2\text{O}_{12}$  and b)  $\text{Li}_6\text{BaLa}_2\text{Ta}_2\text{O}_{12}$  crucibles using reversible metallic lithium electrodes in the frequency range 5 Hz–13 MHz. The measurements were performed inside an argon-filled glove box with an oxygen partial pressure of less than 1 ppm.

the blocking of mobile lithium ions (Fig. 3). The resistance values obtained using AC and direct current (DC) methods using reversible lithium electrodes are nearly the same (Fig. 8), indicating the absence of electrolyte–electrode interface resistance due to the possible formation of interface reaction products, and the conductivity is purely ionic in nature. This observation is consistent with the HW polarization study.

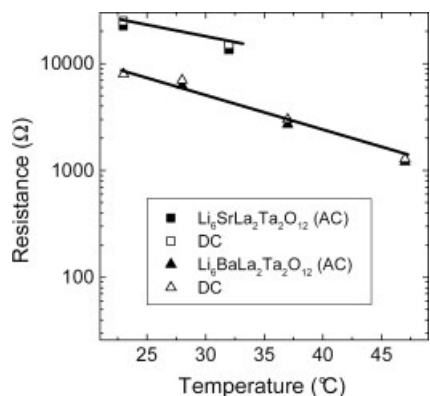


**Figure 8.** Comparison of DC and AC resistance values for  $\text{Li}_6\text{SrLa}_2\text{Ta}_2\text{O}_{12}$  and  $\text{Li}_6\text{BaLa}_2\text{Ta}_2\text{O}_{12}$  crucibles obtained using reversible metallic lithium electrodes. The measurements were performed inside an argon-filled glove box with an oxygen partial pressure of less than 1 ppm. We see that both the AC and DC measurements give similar resistance values, suggesting the absence of electrolyte–electrode interface resistance.

### 2.3. Chemical Reaction Stability with Metallic Lithium

In Figure 9, we show the color of a  $\text{Li}_6\text{BaLa}_2\text{Ta}_2\text{O}_{12}$  crucible (and pellet) after the measurements in contact with molten metallic lithium for a few days, and reveal that the color of the samples did not change after contact with molten elemental lithium. Although we saw a dark color for the corresponding niobium compound, the tantalum compounds were found to be stable against reaction with elemental lithium: A similar mode of behavior is anticipated with perovskite-type lithium ion conductors containing alkaline earth and tantalum.<sup>[24,25]</sup> Accordingly, the investigated materials are considered to be potential electrolytes for all-solid-state lithium batteries.

### 3. Conclusion

We report that the garnet-type  $\text{Li}_6\text{AlA}_2\text{Ta}_2\text{O}_{12}$  ( $\text{A}=\text{Sr}, \text{Ba}$ ) compounds are predominant lithium ion conductors. The materials investigated exhibit mainly a bulk ionic conductivity and high electrochemical stability (decomposition voltages of more than 6 V/Li at room temperature).  $\text{Li}_6\text{BaLa}_2\text{Ta}_2\text{O}_{12}$  shows the highest total lithium ion conductivity of  $4.0 \times 10^{-5} \text{ S cm}^{-1}$  at 22 °C with an activation energy of 0.40 eV, which is comparable to other fast lithium ion conductors. Both the strontium and barium compounds are stable against reaction with molten elemental lithium. The ionic conduction occurs in three-dimensions, similarly to that of other known fast solid lithium ion electrolytes.

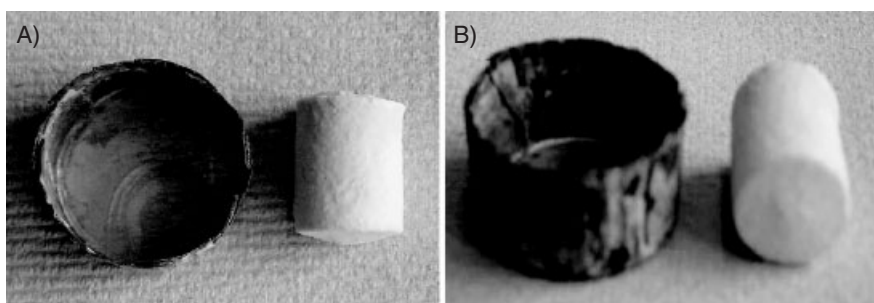


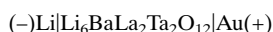
**Figure 9.** Photograph of the  $\text{Li}_6\text{BaLa}_2\text{Ta}_2\text{O}_{12}$  crucible (and pellet) after the reaction with molten lithium (or HW measurements). The A) surface and B) bottom side of the  $\text{Li}_6\text{BaLa}_2\text{Ta}_2\text{O}_{12}$  crucible is shown. (The molybdenum container used for the study is shown along with the sample). A similar observation was observed for corresponding strontium compound,  $\text{Li}_6\text{SrLa}_2\text{Ta}_2\text{O}_{12}$ .

## 4. Experimental

**Material Preparation and Structural Characterization:** Oxides with the chemical formula  $\text{Li}_6\text{ALA}_2\text{Ta}_2\text{O}_{12}$  ( $\text{A}=\text{Sr}, \text{Ba}$ ) were prepared by solid state reaction using stoichiometric amounts of high purity (>99 %) chemicals obtained from Fluka or Aldrich, i.e.,  $\text{La}_2\text{O}_3$  (pre-dried at 900 °C for 24 h),  $\text{LiOH}\cdot\text{H}_2\text{O}$  (10 wt.-% excess was added to compensate for the loss of lithium during annealing),  $\text{Sr}(\text{NO}_3)_2$ ,  $\text{Ba}(\text{NO}_3)_2$ , and  $\text{Ta}_2\text{O}_5$ . The powders were ball-milled using zirconia balls for about 12 h in 2-propanol initially and after heat treatment at 700 °C for 6 h, the reaction products were pressed into pellets by isostatic pressure and annealed at 900 °C for 24 h while the samples were covered with the same mother powder. Powder X-ray diffraction (SEIFERT 3000, Cu K $\alpha$ ) was employed to monitor the phase formation. The lattice constant was obtained by least-squares refinement of the powder XRD data. Calculations of powder XRD patterns was performed using Powder Cell (version 2.3) [11] by substituting strontium at the lanthanum sites (12b) and placing the excess lithium at the  $\text{Li}(1)$ -site (24c) in the space group  $I2_13$ .

**Electrical Characterization:** Electrical conductivity measurements of the pellets ( $\approx 0.15$  cm in thickness and 1 cm in diameter) were performed in air using lithium-ion-blocking gold electrodes (cured at 700 °C for 1 h) in the temperature range 25–300 °C by employing an HP 4192 A Impedance and Gain-Phase Analyzer (5 Hz–13 MHz). Prior to each impedance measurement, the samples were equilibrated for 3 h at constant temperature.

The DC measurements were made on sintered pellets in an argon atmosphere by applying a constant voltage (0–7 V) using gold electrodes. The steady-state current was measured as a function of time using a potentiostat (PG 2.0, Ionic Systems). The Hebb-Wagner polarization measurement was performed inside an argon-filled glove box using a lithium-ion-blocking gold electrode with elemental lithium as the reference electrode [21,22]. A Mo crucible was used to handle the lithium and serve as a current collector. For the HW study, the samples were made in the shape of a crucible ( $\approx 3$  mm in wall thickness, 18 mm in height, 9 mm in outer diameter,  $\approx 4$  mm thick bottom). Before the electrical measurements, the crucible was cycled several times between room temperature and the melting point of lithium. The voltage was applied to the galvanic cell:



The applied voltage will generate a difference in the electronic charge carrier concentration, since no electrostatic potential gradient will be generated. This is the case for a predominant ionic conductor employing a mobile ion blocking electrode, where only the electronic charge carrier will contribute to the steady-state current. The steady-state current density is given by the Hebb-Wagner (HW) equation [22,23] (see Appendix).

**Chemical Reaction Stability With Molten Lithium:** The chemical stability of  $\text{Li}_6\text{ALA}_2\text{Ta}_2\text{O}_{12}$  ( $\text{A}=\text{Sr}, \text{Ba}$ ) with molten lithium was investigated inside an argon-filled glove box by reacting the sample pellet

and/or crucible with a large excess of molten lithium for 3–7 days in the molybdenum crucible. After the heat treatment, the lithium was washed using 2-propanol and water mixtures.

## 5. Appendix

The steady-state current density  $i$  of electrons and holes is given by the Hebb-Wagner equation:

$$i = \frac{kT}{qL} \left[ \sigma_e \left( \exp \left( -\frac{Uq}{kT} \right) - 1 \right) + \sigma_h \left( 1 - \exp \left( \frac{Uq}{kT} \right) \right) \right] \quad (1)$$

where  $k$ ,  $T$ ,  $q$ ,  $L$ , and  $U$  are the Boltzmann constant, absolute temperature, elementary charge, length of the sample (distance between the electrodes) and the applied voltage, respectively. The first term in the brackets approaches a plateau caused by the excess electron conductivity and the second term causes an exponential increase in current due to holes [23,26]. The steady-state current was observed within a few hours ( $\approx 3$  h) and was stable for a long time ( $>3$  days).

Received: February 3, 2004  
Final version: June 18, 2004

- [1] A. D. Robertson, A. R. West, A. G. Ritchie, *Solid State Ionics* **1997**, 104, 1.
- [2] H. Aono, H. Imanaka, G. Y. Adachi, *Acc. Chem. Res.* **1994**, 27, 265.
- [3] G. Y. Adachi, N. Imanaka, H. Aono, *Adv. Mater.* **1996**, 8, 127.
- [4] Y. Inaguma, C. Liquan, M. Itoh, T. Nakamura, T. Uchida, H. Ikuta, W. Wakihara, *Solid State Commun.* **1993**, 86, 689.
- [5] P. Birke, S. Scharner, R. A. Huggins, W. Weppner, *J. Electrochem. Soc.* **1997**, 144, L167.
- [6] a) H. Kawai, J. Kuwano, *J. Electrochem. Soc.* **1994**, 141, L78. b) S. Stramare, V. Thangadurai, W. Weppner, *Chem. Mater.* **2003**, 15, 3974.
- [7] A. F. Wells, *Structural Inorganic Chemistry*, 5th ed., Oxford Science Publications, Clarendon Press, Oxford, UK **1984**.
- [8] H. Hyooma, K. Hayashi, *Mater. Res. Bull.* **1988**, 23, 1399.
- [9] F. Abbattista, M. Vallino, D. Mazza, *Mater. Res. Bull.* **1987**, 22, 1019.
- [10] V. Thangadurai, H. Kaack, W. Weppner, *J. Am. Ceram. Soc.* **2003**, 86, 437.
- [11] W. Kraus, G. Nolze, *J. Appl. Crystallogr.* **1996**, 29, 301.
- [12] R. D. Shannon, *Acta Crystallogr.* **1976**, A32, 751.
- [13] B. A. Boukamp, *Equivalent Circuit*, Version 3.96, 1997, Faculty of Chemical Technology, University of Twente, 7500 AE Enschede, The Netherlands. Reports No: CT88/265/128/CT89/214/128, May **1989**.
- [14] J. T. S. Irvine, D. C. Sinclair, A. R. West, *Adv. Mater.* **1990**, 2, 132.

- [15] V. Thangadurai, R. A. Huggins, W. Weppner, *J. Power Sources* **2002**, *108*, 64.
- [16] H. Y.-P. Hong, *Mater. Res. Bull.* **1978**, *13*, 117.
- [17] X. Yu, J. B. Bates, G. E. Jellison, F. X. Hart, *J. Electrochem. Soc.* **1997**, *144*, 524.
- [18] B. J. Neudecker, W. Weppner, *J. Electrochem. Soc.* **1996**, *143*, 2198.
- [19] W. Weppner, in *Solid State Microbatteries* (Eds: J. R. Akridge, M. Balkanski), Plenum Press, New York **1990**, p. 381.
- [20] M. Casciola, U. Costantino, L. Merlini, I. G. K. Andersen, E. K. Andersen, *Solid State Ionics* **1988**, *26*, 229.
- [21] Y.-W. Hu, I. D. Raistrick, R. A. Huggins, *J. Electrochem. Soc.* **1977**, *124*, 1240.
- [22] C. Wagner, in *Proc. of the 7th meeting of the Int. Committee on Thermodynamic and Kinetic Electrochemistry (CITCE)*, Lindau, Germany, Butterworth Publication, London **1957**, p. 361.
- [23] V. Thangadurai, W. Weppner, *Chem. Mater.* **2002**, *14*, 1136.
- [24] H. Watanabe, J. Kuwano, *J. Power Sources* **1997**, *68*, 421.
- [25] V. Thangadurai, A. K. Shukla, J. Gopalakrishnan, *Chem. Mater.* **1999**, *11*, 835.
- [26] W. Weppner, J. Liu, *Z. Naturforsch.* **1991**, *46a*, 409.